Materials Transactions, Vol. 49, No. 9 (2008) pp. 2147 to 2152

EXPRESS REGULAR ARTICLE

Study on the Reduction of Molybdenum Dioxide by Hydrogen

Byung-Su Kim[1], Eun-young Kim[2], Ho-Suck Jeon[1], Hoo-In Lee[1,*] and Jae-Chun Lee[1]

[1]*Minerals & Materials Processing Division, Korea Institute of Geoscience & Mineral Resources, Daejeon, Korea*
[2]*Department of Resources Recycling, University of Science and Technology, Daejeon, Korea*

The reduction of MoO_2 powder by hydrogen is one of the most important steps for manufacturing ferromolybdenum alloy and molybdenum powder. The results of experiments on the kinetics of this reaction are presented in this paper. The experiments were carried out under nonisothermal condition in hydrogen atmosphere using TGA equipment. The nonisothermal experiments were carried out at various linear heating rates up to 1273 K. It was found that the reduction reaction is very fast under the whole heating rate until the reduction ratio of MoO_2 approaches to about 0.92. The reduction ratio of MoO_2 was about 0.98 after finishing the reduction reaction at a heating rate of 4 K/min. Kinetics of the reaction was analyzed from the dynamic TGA data by means of Coats and Redfern equation. The nucleation and growth model yielded a satisfactory fit to these experimental data. [doi:10.2320/matertrans.MER2008103]

(Received March 27, 2008; Accepted June 25, 2008; Published August 25, 2008)

Keywords: *molybdenum, ferromolybdenum alloy, molybdenum oxides, hydrogen reduction, nucleation and growth model*

1. Introduction

Molybdenum is a refractory metal mainly used as an alloying agent for manufacturing steels, cast irons, and superalloys to increase their mechanical strength, hardness, stiffness, and their resistance to corrosion and wearing. Specially, as an alternative additive of molybdenum in the steel industries, ferromolybdenum alloy which is an alloy of iron and molybdenum has been used primarily.[1)]

The two most common grades of ferromolybdenum alloy are low-carbon ferromolybdenum alloy and high-carbon ferromolybdenum alloy.[1,2)] The high-carbon ferromolybdenum alloy is made by reducing technical grade molybdenum oxide (MoO_3), calcium molybdate ($CaMoO_4$), or sodium molybdate ($NaMoO_4$) with carbon in the presence of iron in an electric furnace (carbon reduction process). The low-carbon ferromolybdenum alloy is more common than the high-carbon alloy, and it is produced by mixing MoO_3, aluminum, ferrosilicon, iron oxide, limestone, lime, and fluorspar, and igniting the aluminum (thermite process). However, in the processes large amounts of slag and dust which cause environmental problems are inevitably generated. Specially, the thermite process uses high cost aluminum and silicon as reducing agents of MoO_3.[3,4)]

Therefore, it would be highly desirable to develop an alternative process to manufacture ferromolybdenum alloy. Generally, the two-step hydrogen reduction process to produce pure molybdenum powders is well known: The first step is to reduce MoO_3 powders to MoO_2 powders at the temperature of below 923 K and the second step is to produce molybdenum powders from MoO_2 powders at the temperature of around 1373 K.[1,5)] Although hydrogen used as a reducing agent of MoO_3 is expensive now, the process has many advantages because slag and dust are not generated in the process and additional additives are not needed. For these reasons, the hydrogen reduction process for manufacturing ferromolybdenum alloy by using MoO_3-iron mixtures was investigated by Gasik and Ostrik.[6)] However, scientific literatures offer little information about kinetic data on the hydrogen reduction process.

The major objective of this research was to determine the kinetics of the reduction of MoO_2 by hydrogen. The kinetics of the reduction reaction would offer fundamental data to understand the influence of employed conditions such as temperature and heating rate on the manufacturing process of ferromolybdenum alloy or molybdenum metal powder. In the present study, a kinetic study on the hydrogen reduction of MoO_2 powder was experimentally investigated under non-isothermal condition using TGA equipment.

2. Thermodynamics

In general, the reaction between MoO_2 and H_2(g) in the hydrogen reduction process to produce molybdenum powders can be represented by

$$MoO_2 + 2H_2(g) = Mo + 2H_2O(g). \quad (1)$$

The standard Gibbs free energy change (ΔG^o) and equilibrium constants (K_1) of the reaction (1) are summarized in Table 1 using HSC Chemistry 5.1 (A. Roine, Outokumpu, 2002) version. The reaction is not favorable thermodynamically under the considered temperature range between 773 and 1273 K since all the ΔG^o values are positive as shown in the table. However, the reaction might take place because the equilibrium constant is relatively large at the temperature range, i.e., the reaction of the hydrogen reduction of MoO_2

Table 1 ΔG^o and K_1 values of the reaction (1).

Temp. (K)	ΔG^o (kJ/mol)	K_1
773	37.1	0.0031
873	30.2	0.0155
973	23.8	0.0530
1073	17.6	0.1386
1173	11.8	0.2990
1273	6.2	0.5575

*Corresponding author, E-mail: hilee@kigam.re.kr

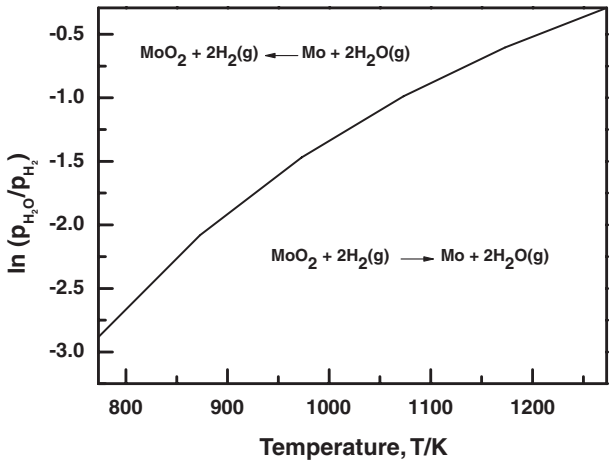

Fig. 1 Plot of $\ln(p_{H_2O}/p_{H_2})$ versus T calculated from the K_1 values of the reaction (1).

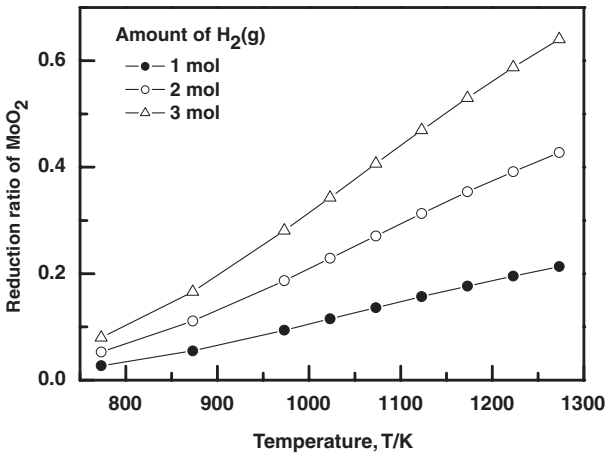

Fig. 2 Reduction ratio of MoO_2 calculated from the equilibrium compositions of the reduction reaction of MoO_2(1 mol) with H_2(g) at a total pressure of 1 atm.

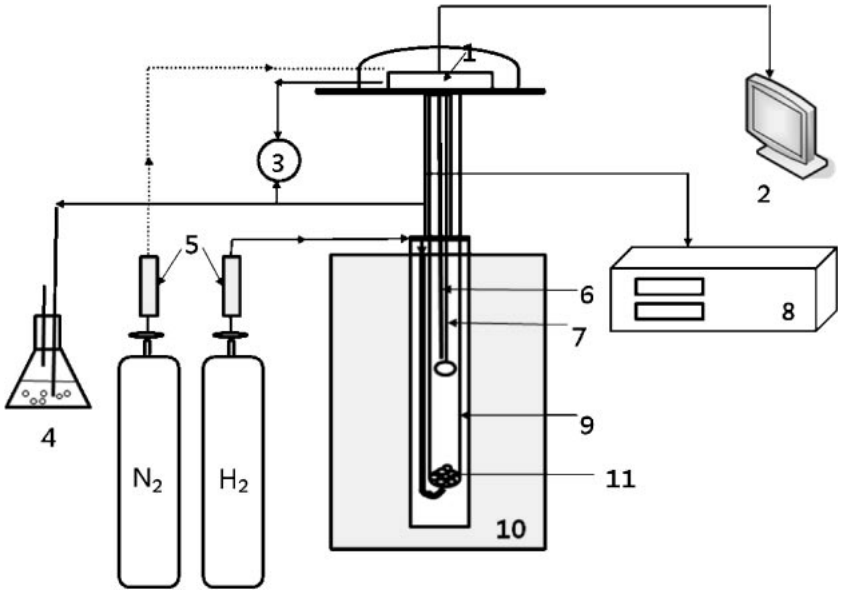

Fig. 3 Schematic diagram of the experimental apparatus for TGA thermal analysis. 1. Micro balance, 2. Data collector, 3. Pressure display, 4. Exhaust gases, 5. Mass flow controller, 6. Thermocouple, 7. Sample tray, 8. Temperature controller, 9. Reactor tube, 10. Furnace, 11. Ceramic ball.

might happen if the partial pressure of water vapor produced from the reaction (1) is relatively low. Figure 1 shows a plot of $\ln(p_{H_2O}/p_{H_2})$ versus T calculated from the K_1 values of the reaction (1). In this figure, the solid line displays the equilibrium state of the reaction (1), and the area below the line indicates that the reaction proceeds to the right side, while the area above the line does that the reaction proceeds to the left side. Thus, Fig. 1 points out the fact that the driving force of the reaction (1) for an arbitrary atmosphere of flue gas in the reaction system increases with increase in the reaction temperature. Figure 2 presents the reduction ratio of MoO_2 calculated from the mass change of oxygen occurred by the reaction of MoO_2 and hydrogen with the amount of hydrogen at the temperature range of 773 to 1273 K. The reduction ratios were obtained by the equilibrium compositions at each temperature calculated using HSC Chemistry 5.1. It is shown in Fig. 2 that the reduction ratio of MoO_2 by hydrogen is relatively low below 900 K compared to that over 900 K. Therefore, it might be expected under a non-isothermal condition that the reaction rate of the hydrogen reduction of MoO_2 will become to be fast at around over 900 K.

3. Experimental

Experiments for measuring the reaction rates of the hydrogen reduction of MoO_2 were carried out in a typical thermogravimetic analysis (TGA) unit. Figure 3 shows a schematic diagram of the apparatus. The apparatus consisted of a recording microbalance from one arm of which a shallow silica tray for MoO_2 powders was suspended by a platinum chain into a reactor tube located within vertical tubular furnace. The reactor tube was an Inconel tube of 5.0 cm i.d. and 65 cm length. The microbalance continuously recorded

the mass changes taking place during the reaction. By means of a gas delivery system, mass flow controllers of hydrogen and nitrogen were also used. The gas temperature in the reactor was measured by chromel-alumel thermocouples. A uniform temperature profile of ±4 K was achieved over 2 cm length of the reaction tube. Dry hydrogen gas was used as a reducing agent, and dry nitrogen was used as an inert gas. A commercial MoO_2 powder (99.0%) of <48 μm size obtained from Aldrich Chemical Co. was used as a raw material.

The experiments were conducted at three heating rates of 4, 8, 12 K/min from room temperature to 1273 K. A sample mass of about 500 mg (±20 mg) of MoO_2 powders was used for each run. During heating, a steady flow of 0.5 L/min of dry hydrogen was maintained through the reactor tube, the microbalance protected from hot gases by flushing it with a dry nitrogen gas of 1 L/min. In order to measure the rates of the hydrogen reduction of MoO_2 in the negligible level of external mass transfer effects, sufficiently high flow rate (0.5 L/min) of hydrogen and bed height (below 1 mm which is obtained by spreading 500 mg of MoO_2 powders as a thin layer on a shallow sample tray) were chosen through preliminary experiments.

The morphological characterization of the samples was performed using a scanning electron microscope (JSM-6380LV, JEOL Ltd, Tokyo, Japan) equipped with an energy dispersive X-ray spectrometer (Link Isis 3.0, Oxford Instrument plc, Oxon, U.K). The XRD patterns were obtained using a X-ray diffractometer (Rigaku D-max-2500PC, Rigaku/MSC, Inc., TX, U.S.A) with Cu Kα radiation ($\lambda = 0.154$ nm) operated at 40 kV and 30 mA. Samples before and after the hydrogen reduction were analyzed by the inductively coupled plasma (ICP) method (JY-38 plus, Horiba Ltd, Kyoto, Japan).

4. Results and Discussion

Figure 4 shows the TGA curve of the hydrogen reduction of MoO_2 obtained at a heating rate of 8 K/min under dry hydrogen atmosphere. The hydrogen reduction pattern obtained at the other heating rates was very similar. It was shown in the figure that the rate of hydrogen reduction of MoO_2 is significantly fast until around 1023 K at which the reduction ratio of MoO_2 is about 0.92. Although not shown here, the reduction ratio of MoO_2 was about 0.98 after finishing the reduction reaction at a heating rate of 4 K/min.

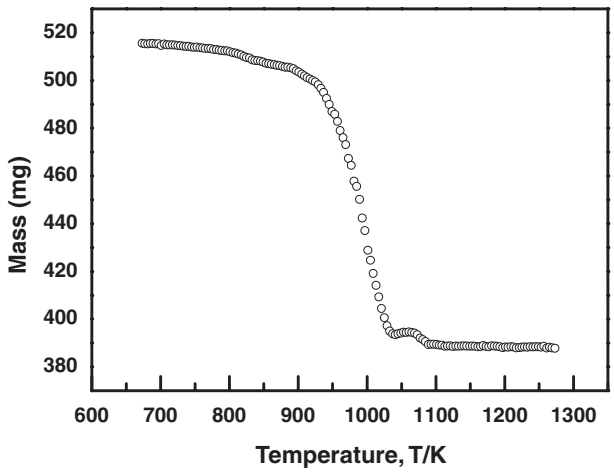

Fig. 4 TGA curve for the reaction of MoO_2 with H_2(g) at a heating rate of 8 K/min in hydrogen atmosphere.

Here, the reduction ratio of MoO_2 powder at a particular temperature during the reduction reaction was determined by dividing the mass change of the solid sample up to that temperature by the total mass change at complete reaction calculated from stoichiometry. It was however found that the rate is very slow during the final stage of reduction. This rate decrease might be the reason why a dense molybdenum shell forms around the particles and subsequently inhibits gaseous transport during the reaction. The phenomenon was indirectly verified by scanning electron microscopy (SEM) analysis of samples before and after heating up to 1273 K. Figure 5 presents the SEM pictures. Figure 5(a) shows a MoO_2 particle before reacting, Fig. 5(b) showing a Mo particle reduced from MoO_2 powder after heating up to 1273 K at a heating rate of 4 K/min. Based on an increase in density during the transformation of MoO_2 to Mo, it is considered that the crystallites grow to form a relatively dense layer, as shown in Fig. 5(b). Thus, Fig. 5 indicates that the surface of Mo particles after reacting is much more impervious than that of MoO_2 particle. Also, the samples before and after reacting were examined by X-ray analysis, which is shown in Fig. 6. XRD pattern of Mo metal was only detected at samples after heating up to 1273 K as shown in the figure.

Kinetic analysis of the thermal data obtained from the reaction of the hydrogen reduction of MoO_2 were done in

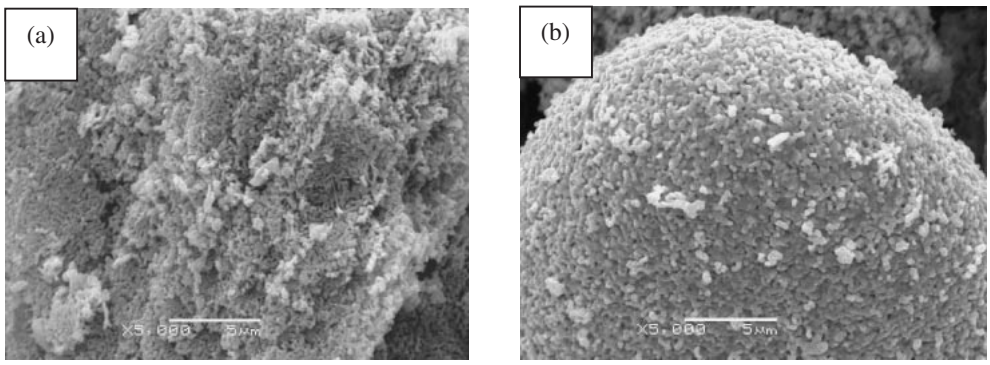

Fig. 5 SEM images of particles before (a) and after (b) heating up to 1273 K.

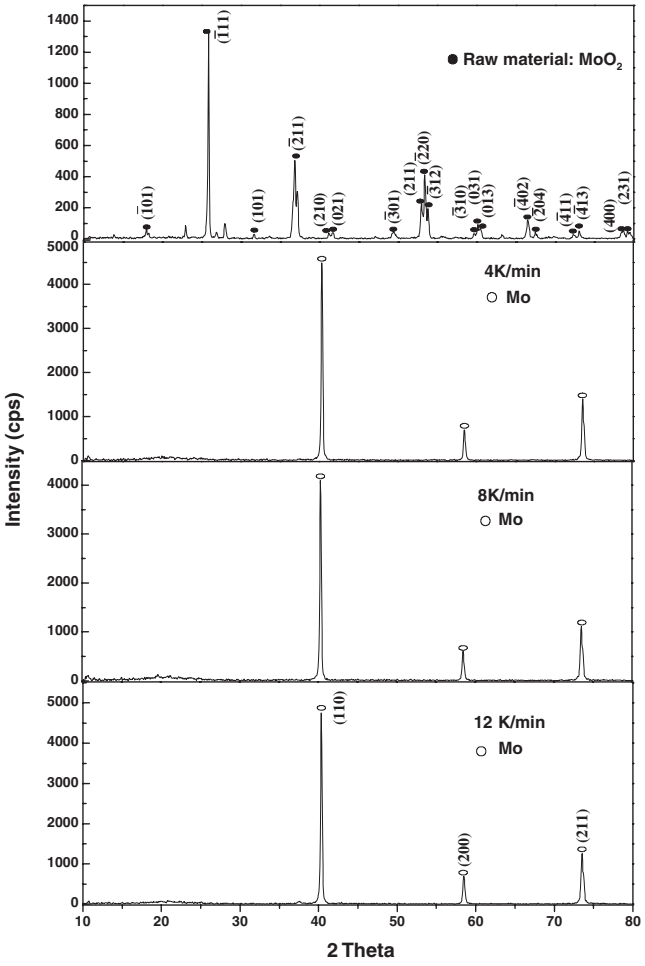

Fig. 6 XRD pattern of the products formed after heating up to 1273 K at various heating rates in hydrogen atmosphere.

order to interpret the mechanism of the reaction and to deduce the kinetic parameters. Figure 7 shows changes in the reduction ratio of MoO_2 with three different heating rates as a function of temperature. In the kinetic analysis, the degree of reduction ratio between 0.12 and 0.92 was investigated. Here, the reduction ratio of MoO_2 was calculated as explained previously. It was shown in Fig. 7 that the rate of the hydrogen reduction of MoO_2 becomes fast at around 900 K, although the reaction temperature is slightly different with heating rate. Such phenomenon could be explained by Fig. 2 that presents the dependence of reaction temperature for the reduction ratio of MoO_2 calculated from equilibrium compositions.

In the present study, kinetic analysis of the reaction rate of the hydrogen reduction of MoO_2 powder under nonisothermal condition was evaluated employing the model fitting method.[7,8] The rate equation can be generally expressed by the following relation:[7–9]

$$\frac{d\alpha}{dT} = \frac{k(T)}{\beta} f(\alpha) \tag{2}$$

where α is the reduction ratio of MoO_2 at temperature T, $f(\alpha)$ the conversion (the reduction ratio of MoO_2) function which is dependent on the mechanism of the reaction, β the heating rate employed in the experiment, and $k(T)$ is the rate constant

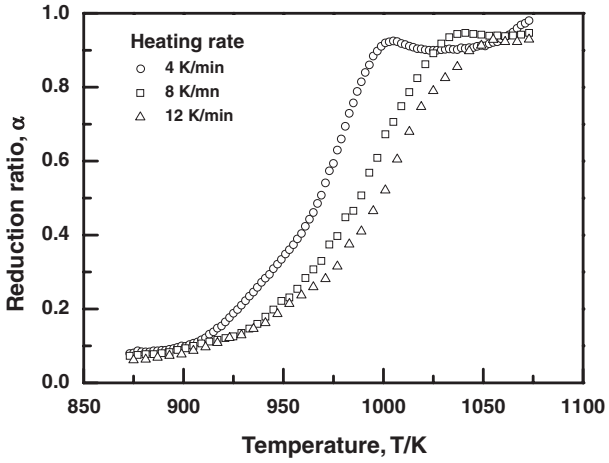

Fig. 7 Changes in the reduction ratio of MoO_2 with three different heating rates as a function of temperature.

as a function of temperature. The temperature dependence of the rate constant is described by the Arrhenius equation,

$$k(T) = A \exp\left(\frac{-E}{RT}\right) \tag{3}$$

where A is the pre-exponential factor (frequency factor), E the activation energy, and R is the gas constant. And, substituting eq. (3) into eq. (2) gives,

$$\frac{d\alpha}{dT} = \left(\frac{A}{\beta}\right) \exp\left(\frac{-E}{RT}\right) f(\alpha). \tag{4}$$

Thus, eq. (4) can be represented by its integral form as follows:[7–9]

$$g(\alpha) = \int_0^{\alpha} \frac{d\alpha}{f(\alpha)} = \int_0^{T} \left(\frac{A}{\beta}\right) \exp\left(\frac{-E}{RT}\right) dT;$$
$$If \ \frac{E}{RT} = x \Rightarrow g(\alpha) = \frac{AE}{\beta R} \int_x^{\infty} \frac{e^{-X}}{x^2} dx. \tag{5}$$

The algebraic expression of the integral $g(\alpha)$ functions that are tested in this work are listed in Table 2.[10–12] These expressions are generally applied for the kinetic analysis of gas-solid state reactions and encompass most common mechanism. However, eq. (5) has no analytic solution, and thus, several approximations were made. One of the most widely used approximations has been given by Coats and Redfern approximation which gives the expression:[7–9]

$$\ln \frac{g(\alpha)}{T^2} = \ln\left(\frac{AR}{\beta E}\left[1 - \frac{2R\bar{T}}{E}\right]\right) - \frac{E}{RT}$$
$$If: \left(\frac{2R\bar{T}}{E}\right) \ll 1 \Rightarrow \ln \frac{g(\alpha)}{T^2} = \ln\left(\frac{AR}{\beta E}\right) - \frac{E}{RT} \tag{6}$$

where $\bar{T}$ is the mean experimental temperature. Thus, eq. (6) was used to analyze the thermal data shown in Fig. 7. It is clear from eq. (6) that a plot of $\ln(g(\alpha)/T^2)$ versus $1/T$ gives a straight line when the adequate $g(\alpha)$ function is chosen. As explained previously, the $g(\alpha)$ function describes the mechanism of the reaction.

The best fit for the thermal data obtained from the reaction of the hydrogen reduction of MoO_2 powder at the reduction ratio range of 0.12 to 0.92 is obtained using nucleation and growth model (A3) with considering all models listed in

Table 2 List of the rate expressions of reaction models used in the study.[10–12)]

Model	Integral form $g(\alpha) = kt$	*Correlation coefficient $= r$
Nucleation and growth models		
Power law (P2)	$\alpha^{1/2}$	>0.97
Power law (P3)	$\alpha^{1/3}$	>0.96
Avarami-Erofe'ev Eq. 1 (A2)	$[-\ln(1-\alpha)]^{1/2}$	>0.97
Avarami-Erofe'ev Eq. 2 (A3)	$[-\ln(1-\alpha)]^{1/3}$	>0.98
Avarami-Erofe'ev Eq. 3 (A4)	$[-\ln(1-\alpha)]^{1/4}$	>0.95
Geometrical contraction models		
Contracting area (R2)	$[1-(1-\alpha)^{1/2}]$	>0.93
Contracting volume (R3)	$[1-(1-\alpha)^{1/3}]$	>0.93
Diffusion models		
1D Diffusion (D1)	α^2	>0.92
2D Diffusion (D2)	$[(1-\alpha)\ln(1-\alpha)]+\alpha$	>0.93
3D Diffusion–Jander Eq. (D3)	$[1-(1-\alpha)^{1/3}]^2$	>0.94
Ginstling-Brounshtein (D4)	$(1-2\alpha/3)-(1-\alpha)^{2/3}$	>0.93
Reaction-order models		
Zero-order (F0/R1)	α	>0.90
First-order (F1)	$-\ln(1-\alpha)$	>0.94
Second-order (F2)	$(1-\alpha)^{-1}-1$	>0.94
Third-order (F3)	$0.5[(1-\alpha)^{-2}-1]$	>0.92

*The correlation coefficients are calculated by fitting the rate data obtained in the experiments into each model equation.

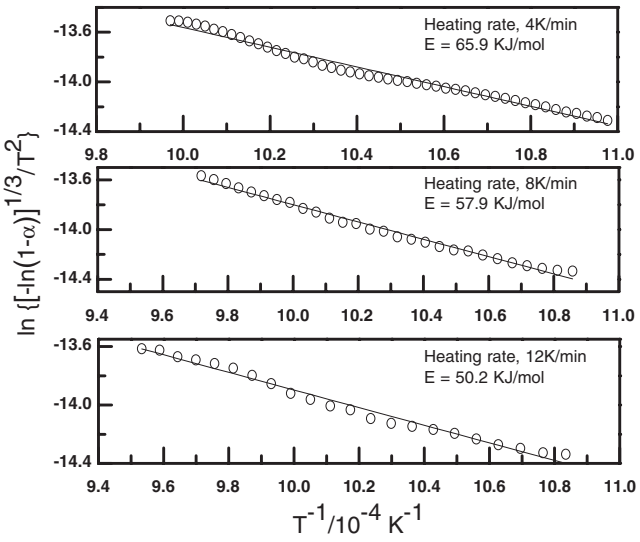

Fig. 8 Plots of $\ln\{[-\ln(1-\alpha)]^{1/3}/T^2\}$ versus $1/T$ using the thermal data of Fig. 7 according to eq. (6).

Table 2, which is shown in Fig. 8. Figure 8 shows plots of $\ln\{[-\ln(1-\alpha)]^{1/3}/T^2\}$ versus $1/T$ using the thermal data of Fig. 7 according to eq. (6). It was thus verified that the nucleation and growth model was applicable as shown in Fig. 8. From Fig. 8, straight lines with high-correlation coefficient ($r > 0.98$) were selected to represent the possible controlling mechanism. Here, the activation energy can be calculated from the slope, the frequency factor from the intercept. The corresponding kinetic parameters are shown in Table 3. Theoretically, the activation energy of a reaction is expected not to change with change in heating rate. But, the activation energy was found to decrease with increase in heating rate, as shown in Table 3. In the study, the reason was not verified. It was only considered that the variation might be deduced to the experimental error. Similarly the frequency factor was also found to be change with heating rate. However, similar trends at nonisotermal condition have been reported in literatures.[8,12,13)] As shown in Table 3, the activation energy of the reaction of the hydrogen reduction of MoO_2 powder was calculated to be 50.2–65.9 kJ/mol, which is similar with that observed in the hydrogen reduction of MoO_3 obtained under stepwise differential isothermal analysis.[6)]

Table 3 Kinetic parameters of the reaction for the hydrogen reduction of MoO_2 powder under nonisothermal condition.

Heating rate (K/min)	E (kJ/mol)	log A/min
4	65.9	4.73
8	57.9	4.10
12	50.2	3.33

5. Conclusion

A kinetic study on the reduction reaction of MoO_2 powder with hydrogen was experimentally investigated under nonisothermal condition using TGA equipment. The experiments were carried out at three heating rates of 4, 8, 12 K/min from room temperature to 1273 K. It was found that the reduction reaction is very fast under the whole heating rate until the reduction ratio of MoO_2 is about 0.92, and after that the rate becomes very slow. The rate decrease might be because a dense molybdenum shell forms around the particles and subsequently inhibits gaseous transport during the reaction. The reduction ratio of MoO_2 was about 0.98 after finishing the reduction reaction at a heating rate of 4 K/min. It was also investigated that the reduction reaction

of the MoO_2 powder by hydrogen follows nucleation and growth model, and the activation energy of the reaction was calculated to be 50.2–65.9 kJ/mol with heating rate.

REFERENCES

1) H. F. Mark *et al.*: *Kirk-Othmer Encyclopedia of Chemical Technology* (America: John Wiley & Sons, vol. 15, 3rd ed., 1981), pp. 670–682.
2) Samsun Logix Corp., Soosong-dong, Seoul, Korea, private communication (February, 2008).
3) K. Jamshidi, H. Abdizadeh, S. A. Seyyed Ebrahimi and K. Hanai: International Journal of Refractory Metals & Hard Materials **22** (2004) 243–245.
4) G. Li, D. Wang, X. Jin and G. Z. Chen: Electrochemistry Communications **9** (2007) 1951–1957.
5) W. V. Schulmeyer and H. M. Ortner: International Journal of Refractory Metals & Hard Materials **20** (2002) 261–269.
6) M. M. Gasik and P. N. Ostrik: J. Thermal Analysis **40** (1993) 313–319.
7) S. Vyazovkin and C. A. Wight: Thermochim Acta **340–341** (1999) 53–68.
8) A. Khawam and D. R. Flanagan: Thermochimica Acta **436** (2005) 101–112.
9) S. Vyazovkin: J. Thermal Analysis **49** (1997) 1493–1499.
10) F. Habashi: *Extractive Metallurgy*, (Gordon and breach, science publishers Inc., **1–2**, 1969) pp. 111–307.
11) P. Pourghahramani and E. Forssberg: Thermochimica Acta **454** (2007) 69–77.
12) P. K. Heda, D. Dollimore, K. S. Alexander, D. Chen, E. Law and P. Bicknell: Thermochimica Acta **255** (1995) 255–272.
13) B. S. Kim, E. Y. Kim, C. K. Kim, H. I. Lee and J. S. Sohn: Mater. Trans., Accepted.